*Biochimica et Biophysica Acta*, 1027 (1990) 105–115
Elsevier



BBAMEM 74952

# Biphasic voltage relaxation pattern observed in cells of *Eremosphaera viridis* after injection of charge-pulses of short duration: detection of tip clogging of intracellular microelectrodes by charge-pulse technique

Günter Wehner, Bruno Friedmann and Ulrich Zimmermann

*Lehrstuhl für Biotechnologie, Würzburg (F.R.G.)*

(Received 21 February 1990)

Key words: Charge pulse; Voltage relaxation; Microelectrode; Tip clogging; (Plant cell)

**Charge pulse experiments performed on the peat-bog alga *Eremosphaera viridis* revealed an unusual voltage relaxation behaviour. Injection of charge pulses of 1 μs duration resulted in an immediate charging of the membranes (time constant of the order of 40 ns). Nevertheless, the potential-measuring microelectrode recorded an exponential increase in membrane voltage with a time constant of about 1.3 ms. The maximum voltage value was recorded after about 3 ms, followed by an exponential decay with a time constant of about 9.6 ms. This biphasic time course was independent of the amplitude of the injected charge and of the location of the impaled microelectrodes in the vacuole. Centrifuged cells in which the chloroplasts and the other organelles were pelleted in one part of the cells showed the same electrical response. Electrical breakdown of the cell membranes resulted in the disappearance of the biphasic voltage response. In this case only the decaying relaxation process could be recorded with a time constant of 3 ms. After resealing of the membranes the original biphasic relaxation response was restored. Increasing concentrations of KCl in the bathing medium reduced both time constants almost correspondingly. The experimental findings were evaluated with an electrical equivalent circuit. Theoretical analysis with reference to the experimental data suggested that the delayed voltage response of the potential-recording electrode resulted from a membrane seal across the tip of this electrode. The resistance of this seal was calculated to be about 400 MΩ. The specific resistances and capacitances of tonoplast and plasmalemma membranes were calculated from the decaying part of the biphasic relaxation curves. The average values were found to be 2.58 $\Omega \cdot m^2$ and 5 $mF \cdot m^{-2}$. The investigations reported here suggest that charge pulse experiments can be generally used for the detection of membrane and cytoplasmic material clogging of the tip of intracellular microelectrodes, a problem with which most electrophysiologists are faced when interpreting data obtained from impaled microelectrodes.**

## Introduction

The charge-pulse technique represents an elegant method for the accurate determination of the electrical properties of biological membranes as well as for the detection of mobile charge transfer through membranes [1–8]. In a charge-pulse experiment the cell membrane is very rapidly charged to an initial voltage by a current pulse of nano- to microsecond duration. The charging circuit contains a diode with a reverse resistance larger than $10^{11}$ Ω. Therefore, the decay of the generated voltage across the membranes can only occur by redistribution of charges within, and ion transport across, the membranes. From the injected charge and the relaxation pattern of the voltage decay the membrane resistance and capacitance as well as the concentration and translocation rate of mobile charges (if present) can be determined [3–8]. In contrast to other electrophysiological methods (current or voltage clamp), the very short pulse-duration of the charge-pulse technique permits the accurate determination of the passive electrical parameters of membranes independent of the magnitude of the resistances in the external measuring circuit. This has the advantage that the relaxation data are straightforward to interpret.

If two membranes are arranged in series (as in plant cells), charge-pulse experiments allow in principle the separate determination of the distinct electrical proper-

Correspondence: U. Zimmermann, Lehrstuhl für Biotechnologie, Röntgenring 11, 8700 Würzburg, F.R.G.

ties of the two membranes (tonoplast and plasmalemma) provided that the specific resistances and capacitances of the membranes differ significantly from each other.

Charge-pulse experiments on giant marine algal cells have emphasized the importance of this technique in the evaluation of the mechanism of sensing of turgor pressure signals and in the subsequent transformation of the pressure signals into ion transport [3–8]. There is evidence that in these algal cells mobile charges of negative sign linked to ion transport systems play a key step in the control of turgor pressure regulation.

In this communication we report analogous charge-pulse experiments on the peat-bog alga *Eremosphaera viridis*. This alga lives in a medium of about pH 5 and shows an unusual morphology. The cell nucleus is centrally located. From the nucleus thin, sometimes branched cytoplasmic strands radiate out through the large vacuole and link up with the thin layer of cytoplasm adhering to the cell wall. The strands and the thin cytoplasmic layers contain chloroplasts.

These algal cells are still large enough (mean diameter about 140 $\mu$m) to introduce microelectrodes and the pressure probe for charge injection and simultaneous recording of the membrane voltage and turgor pressure, respectively [9–13]. *E. viridis* exhibits similar turgor pressure regulation phenomena to marine and littoral algae, but there are also some remarkable differences [13].

The voltage relaxation seen in charge-pulse experiments on *E. viridis* revealed an unusual electrical response after rapid charging of the membrane: a strongly delayed exponential voltage increase followed by an exponential decay of the membrane voltage. The analysis of the data suggests that the potential-recording microelectrode is loosely covered by membrane pieces probably formed by cytoplasmic material during and/or after insertion. Deposition of cytoplasmic and membrane material at the tip and along impaled microcapillaries is always a problem in electrophysiological and intracellular pH measurements. Charge-pulse experiments allow, therefore, direct study of the process of sealing of the intracellular microcapillary tip and measurement of the resistance of this seal.

## Materials and Methods

*Culture of algae. Eremosphaera viridis* de Bary (Algal Culture Collection Göttingen LB 228-1, F.R.G.) was cultivated in a synthetic nutrient solution containing ($\mu$M): 9900 $KNO_3$, 1900 $KH_2PO_4$, 100 $Na_2HPO_4$, 500 $MgSO_4 \cdot 7\ H_2O$, 110 $CaSO_4 \cdot 2\ H_2O$, 130 EDTA, 200 $FeSO_4 \cdot 7\ H_2O$, 180 $H_3BO_3$, 30 $ZnSO_4 \cdot 7\ H_2O$, 7 $MnCl_2 \cdot 6\ H_2O$, 5 $MoO_3$, 10 $CuSO_4 \cdot 5\ H_2O$, vitamins 150 $B_1$ and 730 $B_{12}$ [9]. The temperature was kept at 23° C. The algae suspension was illuminated at 35000 Lux in a light/dark rhythm of 16/8 h. Air, containing 3% $CO_2$, was passed through the culture tubes. The culture medium was changed twice a week. Before experiments coccal cells were selected which did not exhibit cell division. These cells were pre-incubated for about 1 h in a basal medium containing 0.1 mM KCl, 0.1 mM $MgSO_4$, 1 mM $Ca(NO_3)_2$. The pH of the solutions was adjusted to 5.6 with 20.0 mM sodium phosphate buffer.

*Experimental set-up.* The charge-pulse technique has been described in detail in several publications [1–4]. Therefore, we shall give only a short description of the experimental set-up and the special modifications for the application of this technique to the cells of *E. viridis*. Two microcapillaries (prepared from clean lengths of Pyrex glass tubing) were inserted into the cell (Fig. 1). Both microcapillaries were positioned in the vacuole of the given cells (see below). One microcapillary served for injection of the charge (current) pulse and simultaneously for the recording of the turgor pressure, the second one for monitoring the voltage relaxation. In order to avoid irreversible leaks, the tip diameters of the microcapillaries must be small in relation to the diameter of the alga (140 $\mu$m on average). Insertion of the sharp, slightly tapered microcapillaries was achieved using the arrangement shown in Fig. 1. A cell was positioned in a bath of slowly flowing medium at the tip of a glass pipette of about 100 $\mu$m outer tip diameter by application of slight suction generated by a vacuum pump. The current electrode consisted of a 1–2 $\mu$m thick wire of stainless steel of about 10 to 20 mm length moved concentrically through the lumen of a microcapillary with a tip diameter of about 5 $\mu$m. The microcapillary was filled with oil. The wire was connected via a constantan wire to a diode (reverse resistance larger than $10^{11}$ $\Omega$). The diode was connected to a fast pulse generator (Hewlett Packard 214B). The membranes of the cells were charged with a short, rectangular-shaped, positive charge pulse of 1 $\mu$s duration and the injected current was recorded via the voltage drop across a series resistor (1 k$\Omega$) to ground, using an HP 7633 storage oscilloscope. The injected charge $Q$ was determined by planimetry of the area of the stored pulse pattern.

The shank of the microcapillary containing the current electrode was passed through a rubber 'O'-ring in a perspex chamber filled with oil in which a pressure transducer was mounted. The pressure transducer continuously sensed the turgor pressure within the cell in relation to atmospheric pressure provided that the boundary of the cell sap/oil at the tip of the microcapillary was kept constant. This was achieved by displacement of a metal rod inserted perpendicularly through the perspex chamber via a rubber 'O'-ring into the oil. For further description of the pressure probe see the extensive literature on this subject matter [14–16].

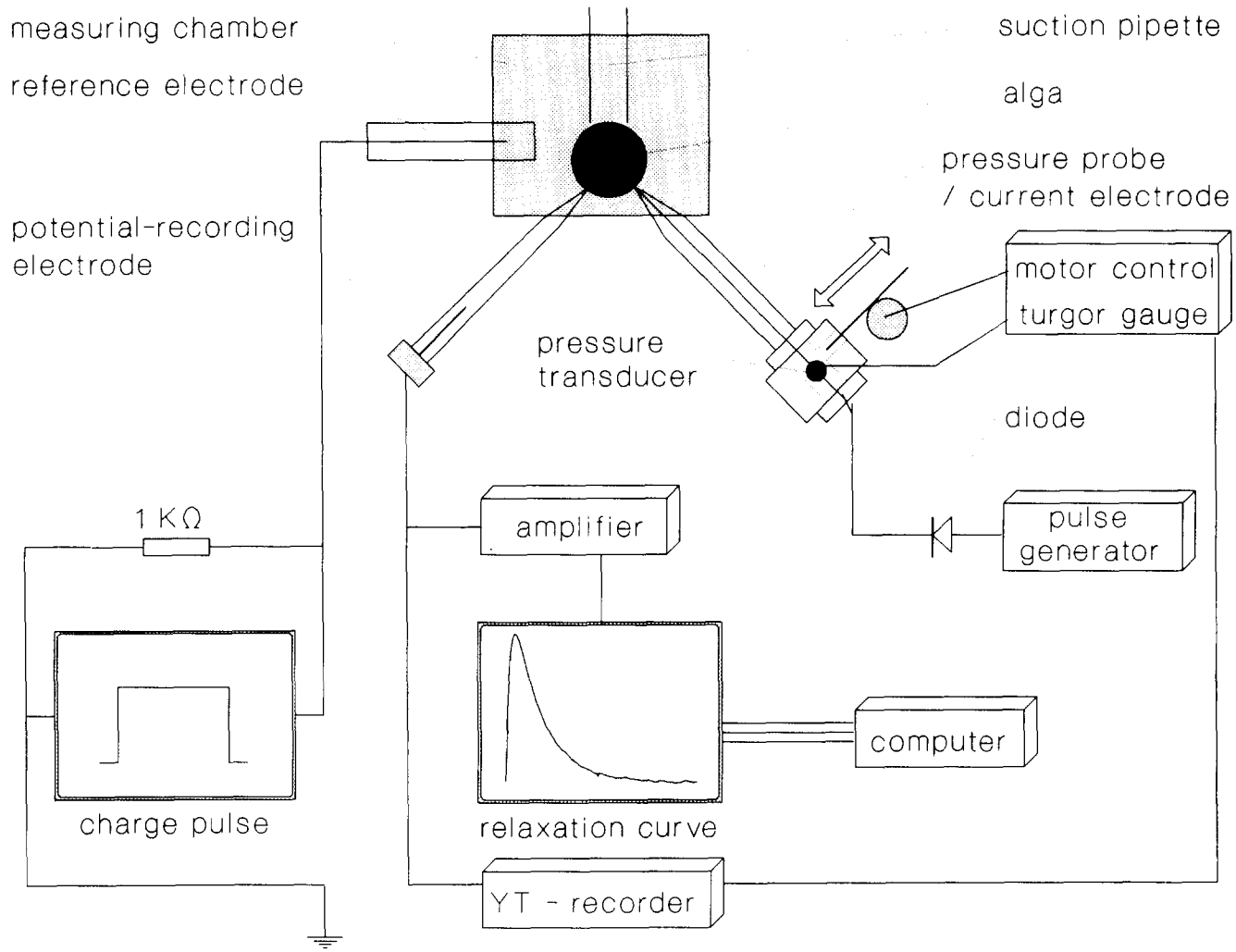


Fig. 1. Assembly for injection of charge pulses and for measuring the voltage relaxation pattern and the turgor pressure in *E. viridis*. For further explanation, see text.

The potential-recording electrode consisted of a microcapillary with a tip-bore diameter of less than 1 $\mu$m. This microcapillary contained an Ag/AgCl-electrode in 150 mM KCl. The potential-recording electrode in combination with the following impedance transformer and the connecting wires had a resistance of about 6 M$\Omega$ and a capacitance of about 3 pF (measured by means of harmonic frequency analysis (Friedmann, Wehner and Zimmermann, manuscript in preparation)). The potential within the cell was measured with respect to a reference Ag/AgCl electrode in the basal medium by an electrometer amplifier with an impedance transformer near the electrode, manufactured in the electronic workshop of the institute. The reference electrode was positioned close to the algal surface. The voltage relaxations were monitored with a digital storage oscilloscope Nicolet 4096A (resolution: 0.5 $\mu$s) or a Tektronix 2440 (resolution: 2 ns) and evaluated with a personal computer. Between charge-pulse experiments the resting membrane potential was recorded with a pen recorder (Philips PM 8221).

## Theoretical considerations

The experimentally measured voltage response of the membranes of *E. viridis* to a charge pulse of 1 $\mu$s duration was biphasic consisting of a strongly delayed, exponential increase followed by an exponential decay (see below). The voltage relaxation pattern can, therefore, be described empirically by the following equation:

$$U_e(t) \approx U_m + U_0(e^{-t/\tau_m} - e^{-t/\tau_d}) \quad (1)$$

$U_e(t)$ is the generated membrane voltage as a function of time $t$. The generated voltage is superposed on the resting membrane potential $U_m$, which can be consid-

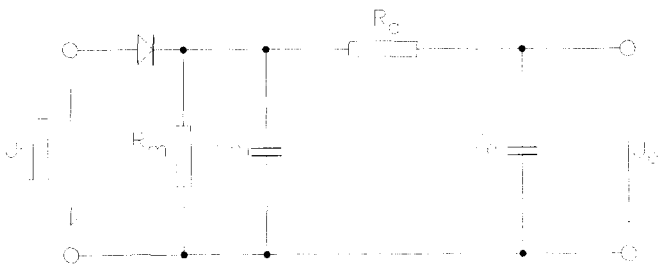

Fig. 2. Electrical equivalent circuit for describing the biphasic voltage relaxation pattern measured after injection of a current pulse into an algal cell of *E. viridis* $R_m$ and $C_m$, specific resistance and capacitance, respectively, of the membrane barrier (tonoplast and plasmalemma). $C_e$, input capacitance of the potential-recording electrode (including the capacitance of the connecting wires and of the input of the amplifier). $R_d$, resistance of the postulated membrane seal at the tip of the potential-recording electrode. $U_i$, input voltage; $U_e$, output voltage.

ered as constant during the charge-pulse experiment. $U_0$ represents the maximum voltage across the membrane, that is theoretically expected from the injected charge. The time constants $\tau_d$ and $\tau_m$ in Eqn. 1 are the relaxation times of the two exponential functions.

Such a biphasic voltage relaxation behaviour is theoretically expected (see Appendix) from an electronic circuit such as shown in Fig. 2. The electronic circuit consists of two low-pass networks $C_m$ in parallel to $R_m$ and the combination of $R_d$ and $C_e$. $C_m$ represents the total membrane capacitance and $R_m$ the total resistance of the tonoplast and plasmalemma membrane barrier. It is assumed that the membrane capacitance is charged *instantaneously* by the charge pulse. Justification for this assumption is obtained by the experimental finding that the correct value for the capacitance of the total membrane barrier can be deduced from the injected charge and the voltage $U_0$. Furthermore, from the values of the total capacity of the cell and of the external resistances (390 pF and about 1000 Ω, see below) the charging time is calculated to be 39 ns.

The time constant of $\tau_m$ controls the charge decay across the membrane and is given by $\tau_m = R_m C_m$ (see Appendix). The treatment of the two membranes (arranged in series) as a single membrane barrier is supported by the experimental finding of only one exponential decaying curve (see below). The following low pass in Fig. 2 consists of the resistance $R_d$ and the capacitance $C_e$ of the potential-recording electrode inclusive amplifier. Thus, the time constant of this network part is given by $\tau_d = C_e R_d$ (see Appendix). The magnitude of $R_d$ controls the delay of recording of the generated voltage which is assumed to be built up instantaneously across the membrane barrier (see above). $R_d$ includes also the electrode resistance which is in series with another larger resistance. This resistance is interpreted as a small section of membrane which loosely seals the tip of the potential-recording electrode. It is presumably formed during and/or after insertion, from cytoplasmic material pushed into the microcapillary or from a flow of membrane material around the tip. Because of the very small area of the tip of the microelectrode the capacitance of this membrane can be neglected and is therefore not included in Fig. 2 and in the following considerations. If the interpretation of $R_d$ in terms of a membrane seal is correct, changes in the resistance of the tonoplast and plasmalemma should be accompanied by corresponding changes of $R_d$ and of $\tau_d$. Changes in membrane resistance can be induced by increase of the electrolyte concentration in the basal medium and also be reversible electrical breakdown of the membranes.

## Results

Measurements were performed about 30 to 40 min after impalement of the potential and current electrodes into the coccal alga *E. viridis*. This time interval was generally sufficient to establish not only a constant membrane potential (−130 mV) and a constant turgor pressure (0.76 MPa), but also to induce a reproducible voltage relaxation pattern (see also below). It should be noted that the resting membrane potential and turgor pressure remained constant during the charging and relaxation experiments. Fig. 3 depicts a typical charge-pulse experiment performed on an algal cell bathed in

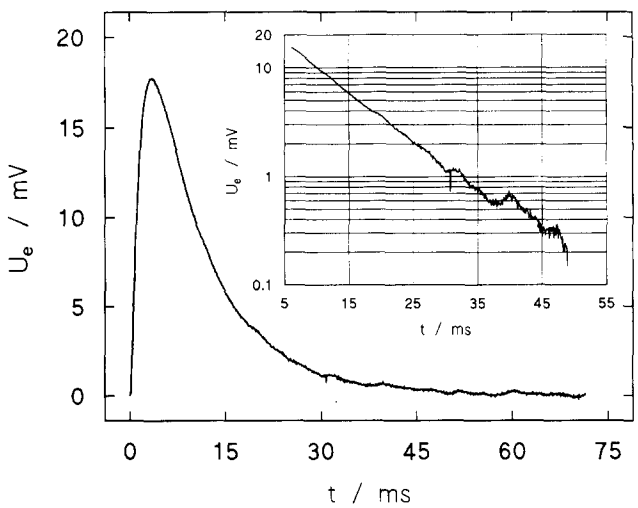


Fig. 3. Biphasic voltage response of a cell of *E. viridis* after injection of a charge pulse of 8 pA·s with 1 μs duration. It is obvious that the membrane voltage, recorded with the microelectrode (tip-bore diameter less than 1 μm) first increased in order to reach a maximum value of 19 mV after about 3 ms. Then the voltage decayed exponentially over the next 50 ms. A semi-logarithmic plot (inset) of the decaying part yields a straight line from which the time constant $\tau_m$ and the initial voltage $U_0$ are calculated to be 9.6 ms and 28.5 mV, respectively (see Theory). The straight line was obtained by fitting the semilogarithmic experimental data using the least-squares method. The algal cell (volume: 1.43 nl, geometric surface area: 0.0613 mm², turgor pressure: 0.76 MPa, resting membrane potential: −130 mV) was bathed in basal medium (pH 5.6), temperature 23° C.

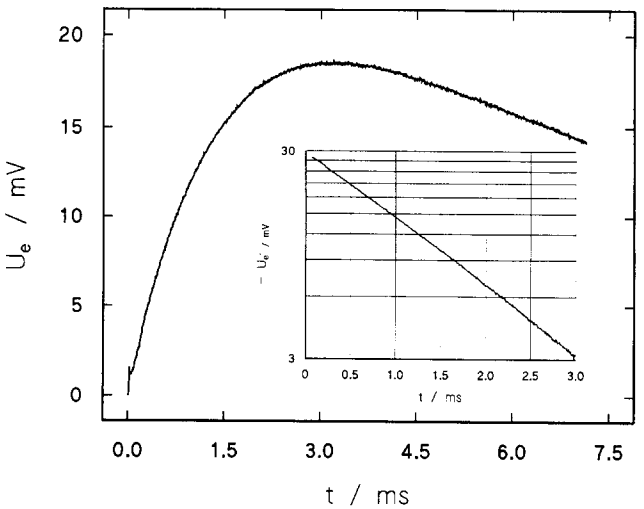


Fig. 4. Voltage relaxation pattern of Fig. 3 displayed at a 10-times higher time resolution in order to analyse the first part of the biphasic voltage response. The inset shows a semilogarithmic plot for which the parameters $\tau_m$ and $U_0$ of the decaying process were subtracted from the experimental curve. The extracted data were again fitted using the least-squares method. The straight line in the semilogarithmic plot (inset) indicates that the increasing part of the biphasic voltage response can also be described by an exponential function. The time constant $\tau_d$ and the final voltage $U_0$ are calculated to be 1.3 ms and 29 mV from the gradient and the intercept, respectively (see Theory). Comparison with Fig. 3 confirms the theoretical prediction that the final voltage of the increasing part of the voltage relaxation pattern is identical with the initial voltage of the decaying part. Note that in this experiment a transient which reflects the injected current pulse was visible.

the basal medium. The membrane capacitance was charged by a current pulse of 1 $\mu$s duration (injected charge, $Q = 8$ pA · s). In contrast to similar experiments on *Valonia utricularis* and *Halicystis parvula* [3–8] the voltage response was delayed considerably. The voltage reached a maximum value after about 3 ms followed by a decay over about 50 ms. The delay in the response after the injection of the 1 $\mu$s charge pulse is obvious from Fig. 4 in which this part of the total relaxation process is displayed with higher time resolution.

The biphasic time course of the voltage measured after injection of a charge pulse can be considered as a superposition of two exponential curves according to Eqn. 1. This is indicated in the insets of Fig. 3 and Fig. 4, in which the two exponential parts of the relaxation curves are plotted on a semi-logarithmic scale. The data points were first fitted by the least-squares method to a straight line of the decaying process (inset of Fig. 3). From the slope of this line the time constant $\tau_m$ was calculated to be $\tau_m = 9.6$ ms, and the initial voltage of the decaying process was found to be $U_0 = 28.5$ mV by extrapolation. Correspondingly, after subtraction of the decaying process the time constant $\tau_d$ of the voltage increase was calculated from the linear fit (inset of Fig. 4) to be $\tau_d = 1.3$ ms and the final voltage (theoretically expected from the injected charge) to be $U_0 = 29$ mV. The experiments show that the final voltage of the increasing process is nearly identical with the initial voltage of the decaying process as it is also true for the two terms of the calculated output signal of the circuit in Fig. 2 (see Appendix, Eqn. 23).

The knowledge of the relaxation times and the initial and final voltages, respectively, allows calculation of the theoretically expected curve of the total time course of the voltage according to Eqn. 1. As shown in Fig. 5 the theoretical curve for the dependence of the voltage on time coincides with the experimental one, indicating that the model discussed above accurately describes the voltage relaxation pattern of *E. viridis*.

From the values for $U_0$ and for the injected charge $Q$, the specific membrane capacitance was calculated from the capacitor equation (see Appendix Eqn. 20) to be $C_m = 5.0$ mF · m$^{-2}$. In terms of the model discussed above (see also Appendix) the relaxation time $\tau_m$ of the decaying process is determined by $R_m$ and $C_m$ (Eqn. 21). Thus, the specific membrane resistance assumed a value of $R_m = 2.53$ $\Omega \cdot m^2$ if the value for $C_m$ derived above is used.

Charge-pulse experiments on 46 different cells yielded an average value of $C_m = 5.0 \pm 1.4$ mF · m$^{-2}$ for the specific membrane capacitance and of $R_m = 2.58 \pm 1.55$ $\Omega \cdot m^2$ for the specific membrane resistance. These values were independent of the amplitude of the injected charge which was varied between 6 and 20 pA · s (corresponding to voltages across the membranes of up to 40 mV). The characteristic time course of the voltage did not change, when the membrane voltage was changed within this range. In addition, no dependence of the

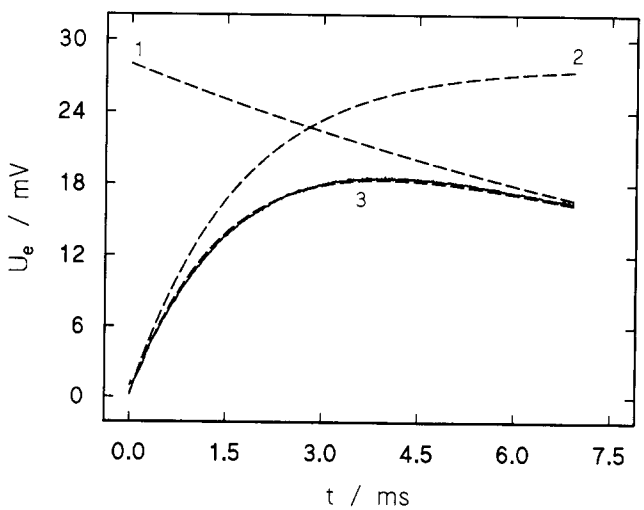


Fig. 5. Theoretical time-dependence of the total biphasic voltage response calculated according to Eqn. 1 using the data for $U_0$, $\tau_m$ and $\tau_d$ of Figs. 3 and 4. As indicated the voltage response is composed of the two exponential curves 1 and 2 (dashed lines). The biphasic voltage response theoretically calculated (curve 3, dashed line) coincides with the experimental response, which exhibits small discontinuities in amplitude (time resolution: 0.5 $\mu$s per point).

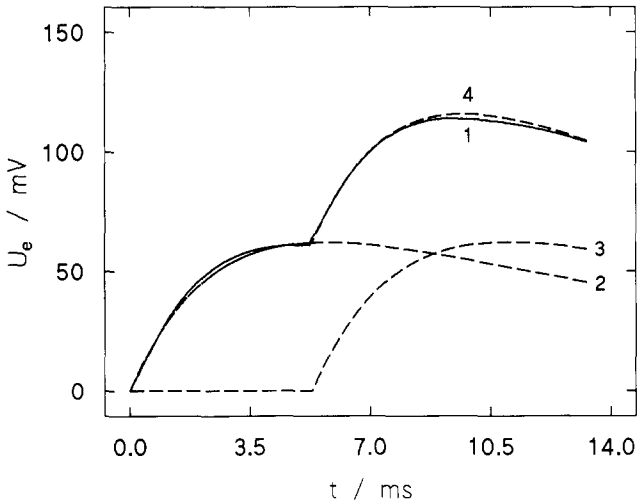


Fig. 6. Curve 1 (solid line) shows the voltage response after sequential injection of two identical 1 μs charge pulses with a delay of about 5 ms. The rising and falling exponentials were used to calculate the parameters $\tau_d$, $\tau_m$ and $U_0$ so that the responses to the pulses applied, individually could be calculated (dashed curves 2 and 3). The sum of these curves (curve 4, dashed) is almost identical to the experimental data (curve 1).

voltage response on the location of the microcapillaries (see Refs. 17, 18) could be detected. This was expected because of the high conductance of the vacuolar sap in relation to the membrane conductance. The strands do not influence the intracellular conductivity because of their very small volume in comparison with the total volume of the vacuole.

Furthermore, injection of a second charge pulse of equal amplitude during the first 4 ms after injection of the first pulse resulted in a linear superposition of the two curves. This is indicated in Fig. 6 where the two separate time courses are graphically superimposed. As expected from the theory it is evident that the increase in voltage across the membrane in response to the second pulse is not influenced by the precharging of the membrane.

Centrifugation of the algal cells at $9600 \times g$ for 8 min before impalement with the microelectrodes also led to no change in the time course of the generated voltage. After centrifugation the chloroplasts and the other organelles were pelleted in one part of the cells whilst the radial cytoplasmic strands appeared intact. The cells were still turgid.

Further investigations on intact cells showed that a constant $C_m$ value could be recorded within a few minutes after impalement with the microelectrodes. However, the time constant $\tau_m$ and therefore the membrane resistance $R_m$ increased until a final value was reached after 30 to 40 min (Fig. 7). Therefore, we have to assume that after impalement of the microelectrodes the specific membrane resistance was low (due to membrane disrupture around the microelectrodes) and then increased with the progress of the resealing process. During these experiments the resting potential remained nearly constant. Sometimes, some fluctuations in the value of the membrane resistance were recorded over longer periods of time even though there were no indications of an irreversible leak in the cell membranes. The occurrence of irreversible leaks resulted in an immediate drop of the turgor pressure and the resting membrane potential.

Simultaneously with the increase of the time constant $\tau_m$ (corresponding to a rising specific membrane resistance $R_m$) as a function of time after insertion, an increase in the time constant $\tau_d$ was also observed (Fig. 7). This is expected in the light of our hypothesis that the resistance $R_d$, which is responsible for the delay in the recorded voltage can be attributed to a membrane seal at the tip. If this membrane seal is formed from cytoplasmatic material pushed into the microcapillary or from the flow of membrane material around the tip, time is required which should be of the same order as that required for the resealing of the membrane area around the impaled microcapillary. Even though $\tau_d$ seemed to assume a constant value after about 40 min pronounced variations in its value afterwards were always observed (Fig. 7) which were much larger than those of the $R_m$. The reason for this could be partly attributed to the larger error in the determination because of the fitting process. However, it is also likely that these fluctuations in the $\tau_d$ values reflected the formation and turnover of the membrane seal and its loose binding to the tip of the microcapillary. The average value of $R_d$ calculated from the average time constant $\tau_d$ (recorded after 30 min impalement) and

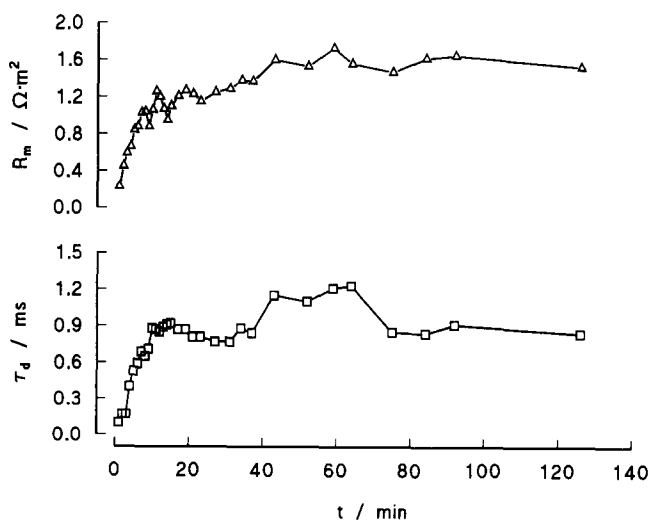


Fig. 7. The membrane resistance $R_m$ (upper curve), calculated from the time constant $\tau_m$ (see Theory) and the time constant $\tau_d$ (lower curve) versus time immediately after insertion of the microelectrode into the cell. Every data point indicates a single charge pulse experiment at the corresponding time. Note, that stationary values are reached after about 40 min, however, that pronounced fluctuations in the value of $\tau_d$ can occur over longer time periods.

TABLE I

*Dependence of the relaxation times $\tau_m$ and $\tau_d$ of a cell of E. viridis (cell-diameter 165.2 μm, cell-surface 0.0855 mm$^2$, cell-volume 2.35 nl) on the external potassium concentrations*

It is obvious that the relaxation times $\tau_m$ and $\tau_d$ and correspondingly $R_m$ and $R_d$ decrease continuously with increasing potassium concentration in the basal medium (BM). Replacement of the KCl-enriched medium by basal medium resulted in the restoration of the original values of $\tau_m$ and $\tau_d$. Note that the resting potential decreased in proportion to the increase of the KCl concentration in the external medium. For further explanations see text.

| Medium | $\tau_d$ (ms) | $\tau_m$ (ms) | $R_m$ ($\Omega \cdot m^2$) | $C_m$ ($mF \cdot m^{-2}$) | $R_d$ ($M\Omega$) |
|---|---|---|---|---|---|
| BM | 2.05 | 8.94 | 2.01 | 4.5 | 683 |
| 3 mM KCl | 1.38 | 6.08 | 1.30 | 4.7 | 460 |
| BM | 2.11 | 8.63 | 2.12 | 4.1 | 703 |
| 10 mM KCl | 1.22 | 3.07 | 0.83 | 3.7 | 407 |
| BM | 1.82 | 9.88 | 2.03 | 4.9 | 607 |
| 20 mM KCl | 0.77 | 2.65 | 0.60 | 4.4 | 257 |
| BM | 1.97 | 8.48 | 2.04 | 4.2 | 657 |
| 30 mM KCl | 0.68 | 2.39 | 0.49 | 4.9 | 227 |
| BM | 1.79 | 7.57 | 1.75 | 4.3 | 566 |

using an electrode input capacitance of $C_e = 3$ pF (see Theory) was about 400 MΩ.

The interpretation of $R_d$ in terms of a loose membrane seal is consistent with the observation that the relaxation time $\tau_d$ decreased when the membrane resistance was decreased by increasing the electrolyte concentration in the external medium. Table I represents results of experiments in which an algal cell was bathed in basal medium (BM) supplemented with 3, 10, 20 or 30 mM KCl. In the presence of increasing concentrations of potassium the measured parameters $\tau_d$, $\tau_m$ and the calculated values for $R_m$ and $R_d$ are lowered reversibly. This is expected due to the changes in intracellular KCl because of osmotic processes.

Dramatic, but still reversible, changes in membrane resistance can also be induced by electrical breakdown of the cell membrane [19,20]. Reversible electrical breakdown requires the injection of charge pulses of high amplitude and of μs duration. Breakdown of the membranes of *E. viridis* occurred when the generated membrane voltage exceeded 300 to 600 mV (Fig. 8). The variation of the breakdown voltage from cell to cell is unusual, compared with analogous studies on other plant and mammalian cells [19,20] and is not understood at present. It is conceivable that the variation arises from voltage-dependent potassium channels [11] which may be open at higher membrane voltages. Support for this assumption is provided by curve 4 in Fig. 8, which indicates that the time constants $\tau_d$ and $\tau_m$ change their magnitude if the voltage exceed 500 mV. However, in all cases analysis of the discharging process showed that the specific membrane resistance dropped instantaneously to very low values. Relaxation measure-

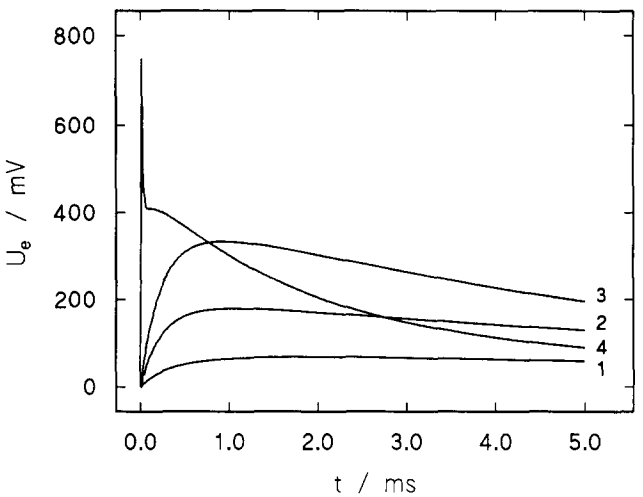


Fig. 8. Voltage response (curve 1–4) versus time for increasing amplitudes of the charge pulses (27, 55, 75, 150 pA·s). When the electrical breakdown voltage is exceeded (about 500 mV) during the charge pulse application (curve 4) the potential across the membrane dropped immediately to low values.

ments performed immediately after electrical breakdown had indicated that the first exponential curve had disappeared. Only the exponential decaying process could be recorded.

Immediately after breakdown the voltage relaxation of the membranes of *E. viridis* is described analogous to other algal cells by the usual electrical network consisting of a membrane resistance $R_m$ in parallel to the membrane capacitance $C_m$ (Fig. 2). As resealing of the membrane proceeded $\tau_m$ and $\tau_d$ increased until the original values were reached.

Further evidence for the hypothesis of a membrane seal at the tip of the potential-recording electrode was obtained by investigations of the voltage behaviour of

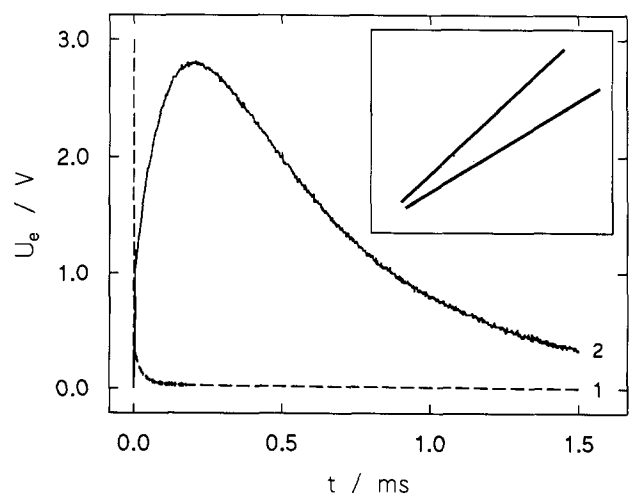


Fig. 9. Voltage response of a charge pulse outside the cell in the basal medium (curve 1, dashed line). After formation of a KCl-crystal in the tip of the microcapillary by drying a microelectrode (see inset) it is evident that the time constants of the biphasic curve were increased significantly.

this electrode monitored outside the cell. Because of the small capacity of the electrode voltages in the volt range must be built up for resolution of the relaxations. Fig. 9 (curve 1) shows the typical voltage relaxation of a potential-recording electrode used for the measurements mentioned above. The presence of a crystalline particle in the tip of the microcapillary (see inset of Fig. 9) resulted in a biphasic voltage relaxation analogous to conditions in the microelectrode normally impaled in *E. viridis* cells (Fig. 9, curve 2). However, the maximum voltage of curve 2 (Fig. 9) was recorded after 0.25 ms, indicating that the tip was only loosely clogged.

## Discussion

The apparently biphasic voltage relaxation pattern observed experimentally in *E. viridis* can be explained by the assumption that the tip of the potential-recording electrode is covered or clogged by membrane material. It is well-known that as a microelectrode is inserted into a plant cell, the turgor pressure forces vacuolar sap into the tip, thus displacing any cytoplasm surrounding the tip [21,22]. However, the cytoplasm can subsequently creep along the microelectrode which had been inserted into the vacuole and eventually flow over the tip. Similar phenomena can be assumed to occur in impaled cells of *E. viridis*.

Several considerations show that there is no reasonable doubt that both microcapillaries were positioned in the vacuole of *E. viridis*. First, the cytoplasmic layer is very thin. Therefore, the tip diameter of the microcapillary used for combined injection of charge pulses and the measurement of the turgor pressure was too large for positioning in the cytoplasmic layer. In addition, the wire used for the injection of the charge pulse was pushed through the tip by about 50 $\mu$m and must therefore be positioned in the vacuole of *E. viridis*. A possible deposition of cytoplasmic or membrane material along the wire also seems to be unlikely, even though it cannot be completely excluded. However, if this happened there would be no effect on the injection of charge pulses. Taking the very small surface area of the wire outside the tip (about $10^{-10}$ m$^2$) and the high current (10 $\mu$A) into account it can easily be calculated that the breakdown voltage of a membrane piece covering the tip of this microcapillary is exceeded even by charge pulses of very low amplitudes. In addition, there is good evidence that the large tip of this current/pressure-microcapillary was not clogged by cytoplasmic or membrane material. Displacement of the metal rod showed that the boundary cell-sap/oil was easily moved indicating that the tip of this microcapillary was completely free. This suggests that the tip of this microcapillary was also inside the vacuole or, at least, that the wire prevented the clogging of the tip. In the case of the potential-recording microcapillary (bore at the tip less than 1 $\mu$m) it is also very unlikely that the tip remained in the thin cytoplasmic layer (see Ref. 23).

In contrast to results obtained on *Valonia ventricosa* [24,25] it is important to note that we have convincing evidence that the potential-recording microelectrode was positioned within the vacuole. The value of 5 mF $\cdot$ m$^{-2}$ for the total specific membrane capacitance calculated from the injected charge and the corresponding initial voltage can be only explained if two membranes were arranged in series to each other. The specific capacitance of a unit membrane is between 7 and 13 mF $\cdot$ m$^{-2}$ [26–31]. Smaller values than 7 mF $\cdot$ m$^{-2}$ were never reported and apparent values higher than 13 mF $\cdot$ m$^{-2}$ were only recorded in the presence of mobile charges [2,3,7] or of folded membranes [32,33]. With an average value of 10 mF $\cdot$ m$^{-2}$ for the specific capacitance of the unit membrane a total specific capacitance of 5 mF $\cdot$ m$^{-2}$ is expected if the potential-recording microelectrode was located in the vacuole. This calculation assumes that both membranes have the same area as determined from the geometric dimensions under the microscope. Due to the strands crossing the vacuole the tonoplast surface of *E. viridis* may be enlarged by a factor of 1.5 to 2. In this case the specific capacitance of both membranes could assume a value of 7 mF $\cdot$ m$^{-2}$ which implies an apparent tonoplast capacity of 10.5 to 14 mF $\cdot$ m$^{-2}$. These values are still in the range reported in the literature. At first glance the intracellular pH measurements of Steigner et al. [12] in *E. viridis* are in contradiction to this conclusion. These authors measured a pH value of 7.0 to 7.8 and claimed that this value is consistent only with the assumption that the pH microelectrode (bore at the tip less than 1 $\mu$m) was located within the cytoplasm [34]. In the studies of Steigner et al. [12] tip clogging should be dramatic because simple microelectrodes were used which were not pressure-tight.

The electrical breakdown measurements performed in this work also support the view that the tip of the potential-recording electrode was covered by a membrane and not by unstructured material. This can be concluded from the finding that the delaying resistance $R_d$ introduced by the electronic circuit exhibits the same electrical features in response to breakdown as intact biological membranes [19,20]. Breakdown could be repeated several times after subsequent resealing of the structure with simultaneous restoration of the original resistance value. Such effects can only be expected if we are dealing with membranes consisting of lipid bilayer structures. The effect of electrical breakdown on $\tau_d$ also excludes the possibility that the resistance $R_d$ in the electronic circuit of Fig. 2 reflects the resistance of the cell wall and/or of the 0.1 $\mu$m thick layer of mucus around the cells [13]. Such layers do not exhibit a reversible breakdown [19,20]. A loose membrane seal at

the tip also explains the finding that the biphasic response was still present in centrifuged cells.

The result that the values of both resistances $R_m$ and $R_d$ showed the same trend with increasing KCl concentration in the external medium also supports the conclusion that the delaying resistance $R_d$ reflects the resistance of a membrane (see discussion above).

Convincing support for membrane formation at the tip of the potential-recording electrode is also given by the experiments in which the voltage response of this electrode was monitored outside the cells (Fig. 9). After formation of a KCl crystal in the tip of the microcapillary the time constant of the rising exponential was increased to 0.1 ms. This value is still significantly less than that observed when the microcapillary was impaled in the cell. This indicates that under the latter condition the tip must be sealed by a membrane or clogged by very dense membrane-like material.

The assumption of a loose membrane seal around the tip is not inconsistent with reports on deposition of cytoplasmic material along the microcapillary because it is well known that cytoplasmic material can very easily form membrane sheets and vesicles if it is disturbed [35–38]. We cannot yet decide if this membrane material at the tip of the microelectrode results from cytoplasm pushed into the microcapillary by turgor pressure during insertion or by subsequent flowing of tonoplast membrane over the tip when placed in the vacuole. In the latter case we must assume that the original tonoplast still insulated the tip of the microelectrode in the vacuole from the cytoplasmic layer in order to give the total capacitance value of two membranes in series.

Further evidence that our interpretation of the data in terms of the electronic circuit in Fig. 2 is appropriate comes from the finding that the total specific resistance of $2.58 \pm 1.55\ \Omega \cdot m^2$ calculated from the decaying part of the relaxation curves is nearly identical to the value of $2.7 \pm 2.1\ \Omega \cdot m^2$ measured by Köhler et al. [10] by means of a single-electrode double-pulse current-clamp technique [39]. The agreement of the values also indicates that conventional electrophysiological methods yield the right value for the resistance provided that the measurements were performed in the 'quasi-stationary state'. As shown here tip clogging becomes only effective on voltage relaxations.

In the light of our arguments presented above the mean value of the membrane resistance of $2.58\ \Omega \cdot m^2$ most probably reflects the total value of the two membranes arranged in series. The resolution of the charge pulse technique is 5 $\mu$s [1–8]. However, due the delayed potential recording in *E. viridis* the decaying process can only be monitored after about 3 ms. Thus, the tonoplast resistance must be at least $0.6\ \Omega \cdot m^2$ or higher to be resolved. The finding that the voltage decay could be fitted by only one exponential curve suggests either that both membranes have nearly identical electrical properties or that the time constant of the tonoplast is below 3 ms. The latter explanation would imply that the tonoplast membrane is fairly conductive. Even though Lainson and Field [24] claim that the tonoplast of *V. utricularis* has a low resistance, most of the data so far obtained on isolated vacuoles suggest high tonoplast resistances [40,41].

The question with regard to the existence of mobile charges in the membranes of *E. viridis* cannot be answered at the present. Due to the delayed response of the potential-recording electrode the relaxation process arising from mobile charges if present is masked. In addition, because of the low pH value of the basal medium it cannot be excluded that any mobile charges in the membranes of *E. viridis* are neutralised (if they bear a negative charge as is the case of *V. utricularis* and *H. parvula*).

To summarize, the present communication points out that the charge pulse relaxation technique can be used for the detection of membrane and cytoplasmatic material clogging of the tip of microelectrodes, a problem with which most plant electrophysiologists are faced when interpreting data obtained from implanted microelectrodes. The effect of delayed potential-recording is most dramatic in *E. viridis*, but should also be present in other algal and plant cells. Preliminary high resolution charge pulse measurements on the internodes of *Nitella* species also indicate a delay in potential response, although this is shorter than in *E. viridis*.

## Appendix

The biphasic voltage relaxation pattern observed in charge pulse experiments on *E. viridis* can be described by the electronic circuit in Fig. 2. For analysis it is convenient to transform this network into the circuit of Fig. 10. This transformation is justified by the experimental finding that the current electrode charges the membrane capacitance $C_m$ to the initial voltage $U_0$ very

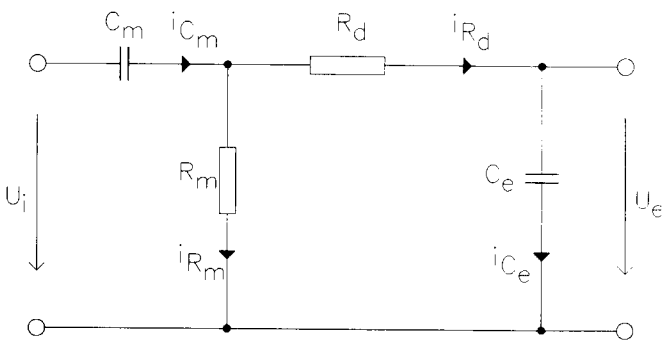


Fig. 10. Equivalent circuit transformed from Fig. 2. In this circuit the instantaneously charged capacitance $C_m$ is replaced by a voltage source $U_i$ and an uncharged capacitance. The currents are denoted by $i$, otherwise the symbols have the same meaning as in Fig. 2. For further details, see Appendix.

rapidly compared to the time of potential-recording. Therefore, according to electrical network theory [42] this precharged capacitance is equivalent to a direct voltage source arranged in series with an uncharged capacitance, Fig. 10. Thus, in this circuit the charge pulse is replaced by a voltage signal which is a step function. The magnitude of this step function is equal to the voltage $U_0$ generated across the capacitor $C_m$ after the application of the charge pulse. Application of Kirchhoff's laws to this circuit yields the following primary equations:

$$i_{Cm}(t) = i_{Rd}(t) + i_{Rm}(t) \tag{2}$$

$$i_{Rd}(t) = i_{Ce}(t) \tag{3}$$

$$U_i(t) = u_{Cm}(t) + u_{Rd}(t) + U_e(t) \tag{4}$$

$$u_{Rm}(t) = u_{Rd}(t) + U_e(t) \tag{5}$$

which describe the currents $i$ and voltages $u$ in the circuit (printed in lower cases). For the meaning of the subscripts, see Figs. 2 and 10. The relationships between the voltages and currents are given by:

$$i(t) = C \cdot \mathrm{d}u/\mathrm{d}t \tag{6}$$

$$u(t) = R \cdot i(t) \tag{7}$$

The introduction of Eqns. 6 and 7 into Eqns. 2–5 yields a set of linear differential equations with constant coefficients.

This set of equations can be Laplace transformed. The input voltage $U_i(t)$ and the output voltage $U_e(t)$ of the network are transformed into the frequency domain. It is appropriate to express the Laplace parameter $s$ as a complex operator which includes the frequency. The Laplace transformation of Eqns. 6 and 7 into the frequency domain is given by:

$$i(s) = sCu(s) \tag{8}$$

$$u(s) = Ri(s) \tag{9}$$

With these relationships the currents and voltages in the circuit of Fig. 10 can be described as follows:

$$i_{Cm}(s) = sC_m u_{Cm}(s) \tag{10}$$

$$i_{Rm}(s) = u_{Rm}(s)/R_m \tag{11}$$

$$i_{Rd}(s) = u_{Rd}(s)/R_d \tag{12}$$

$$i_{Ce}(s) = sC_e u_{Ce}(s) \tag{13}$$

Combination of these equations and algebraic manipulation leads finally to the following transfer function:

$$\frac{U_e(s)}{U_i(s)} = \frac{s/R_d C_m}{s^2 + s\left[\frac{1}{R_d C_m} + \frac{1}{R_d C_e} + \frac{1}{R_m C_m}\right] + \left[\frac{1}{R_m C_m R_d C_e}\right]} \tag{14}$$

As mentioned above, the input signal $U_i(s)$ is assumed to be a step function described in the frequency domain as $U_0/s$. The output signal $U_e(s)$ is therefore:

$$U_e(s) = \frac{U_0/R_d C_m}{s^2 + s\left[\frac{1}{R_d C_m} + \frac{1}{R_d C_e} + \frac{1}{R_m C_m}\right] + \left[\frac{1}{R_m C_m R_d C_e}\right]} \tag{15}$$

Retransformation of Eqn. 15 [43] yields the output function in the time domain. To this end we have to calculate the poles $\alpha_{1,2}$ of Eqn. 15, which are:

$$\alpha_{1,2} = \left[\frac{1}{2R_d C_m} + \frac{1}{2R_d C_e} + \frac{1}{2R_m C_m}\right] \pm \left[\left[\frac{1}{2R_d C_m} + \frac{1}{2R_d C_e} + \frac{1}{2R_m C_m}\right] - \left[\frac{1}{R_m C_m R_d C_e}\right]\right]^{1/2} \tag{16}$$

These poles correspond to the reciprocal time constants $\alpha_1 = 1/\tau_d$ and $\alpha_2 = 1/\tau_m$ of the network plotted in Fig. 2.

With Eqn. 16 the retransformation of Eqn. 15 into the time domain yields then the following function:

$$U_e(t) = U_0 \frac{\tau_m}{(\tau_m - \tau_d)} (e^{-t/\tau_m} - e^{-t/\tau_c}) \tag{17}$$

with a maximum at:

$$t_m = \frac{\tau_m \tau_d}{\tau_m - \tau_d} \ln(\tau_m/\tau_d) \tag{18}$$

Inspection of Eqn. 17 indicates that the amplitude $U_a$, defined as

$$U_a = U_0 \frac{\tau_m}{(\tau_m - \tau_d)} \tag{19}$$

not only represents the initial amplitude of the declining term but also the final amplitude of the increasing term. However, these amplitudes are not necessarily equal to the voltage $U_0$ to which the capacitance is initially charged.

Eqns. 15–19 and the capacitor equation

$$Q = C_m U_0 \tag{20}$$

entirely describe the network in Fig. 2. These equations represent a transcendental set of equations which cannot be solved analytically.

However, the experiments show that $C_e$ is much smaller than $C_m$. With this approximation we get from Eqn. 16 the simplified and independent time constants:

$$\tau_m = R_m C_m \tag{21}$$

$$\tau_d = R_d C_e \tag{22}$$

The experimental results yield furthermore that for *E. viridis* the relation $\tau_m > \tau_d$ is valid under all experimen-

tal conditions. Hence, it follows from Eqn. 19 the condition $U_a \approx U_0$ in agreement with the analysis of the experimental findings. With this in mind we can rewrite Eqn. 17 as follows:

$$U_e(t) = U_0(e^{-t/\tau_m} - e^{-t/\tau_d}) \quad (23)$$

Eqn. 23 is identical to the empirically derived Eqn. 1 in the section 'Theoretical considerations', if we take into account that the generated potential $U_e(t)$ is superposed on the resting membrane potential $U_m$ which is assumed to be constant.


## Acknowledgements

The authors are grateful to Prof. R. Benz and Dr. W.M. Arnold for stimulating discussions. This work was supported by a grant of the Sonderforschungsbereich 176 (Project B4) to U.Z.


## References


1 Benz, R. and Läuger, P. (1976) J. Membr. Biol. 27, 171–191.
2 Benz, R. and Conti, F. (1981) J. Membr. Biol. 59, 91–104.
3 Zimmermann, U., Büchner, K.-H. and Benz, R. (1982) J. Membr. Biol. 67, 183–197.
4 Benz, R. and Zimmermann, U. (1983) Biophys. J. 43, 13–26.
5 Büchner, K.-H., Rosenheck, K. and Zimmermann, U. (1985) J. Membr. Biol. 88, 131–137.
6 Büchner, K.-H., Walter, L. and Zimmermann, U. (1987) Biochim. Biophys. Acta 903, 241–247.
7 Benz, R., Büchner, K.-H. and Zimmermann, U. (1988) Planta 174, 479–487.
8 Walter, L., Büchner, K.-H. and Zimmermann, U. (1988) Biochim. Biophys. Acta 939, 1–7.
9 Köhler, K., Geisweid, H.-J., Simonis, W. and Urbach, W. (1983) Planta 159, 165–171.
10 Köhler, K., Steigner, W., Simonis, W. and Urbach, W. (1985) Planta 166, 490–499.
11 Köhler, K., Steigner, W., Kolbowski, J., Hansen, U.-P., Simonis, W. and Urbach, W. (1986) Planta 167, 66–75.
12 Steigner, W., Köhler, K., Simonis, W. and Urbach, W. (1988) J. Exp. Bot. 39, 23–36.
13 Frey, N., Büchner, K.-H. and Zimmermann, U. (1988) J. Membr. Biol. 101, 151–163.
14 Zimmermann, U., Räde, H. and Steudle, E. (1969) Naturwissenschaften 56, 634.
15 Zimmermann, U. and Steudle, E. (1978) Adv. Bot. Res. 6, 45–117.
16 Zimmermann, U. (1989) Methods Enzymol. 174, 338–366.
17 Purves, R.D. (1976) J. Theor. Biol. 63, 225–228.
18 Peskoff, A. and Ramirez, D.M. (1975) J. Math. Biol. 2, 301–316.
19 Zimmermann, U. (1982) Biochim. Biophys. Acta 694, 227–277.
20 Zimmermann, U. (1986) Rev. Physiol. Biochem. Pharmacol. 105, 175–256.
21 Walker, N.A. (1955) Aust. J. Biol. Sci. 8, 476–489.
22 Findlay, G.P. and Hope, A.B. (1976) in Transport in Plants II, Part A, Cells (Lüttge, U. and Pitman, M.G., eds.), pp. 53–92, Springer-Verlag, Berlin.
23 Spanswick, R.M. (1970) J. Exp. Bot. 21, 617–627.
24 Lainson, R. and Field, C.D. (1976) J. Membr. Biol. 29, 81–94.
25 Davis, R.F. (1981) Plant Physiol. 67, 825–831.
26 Fricke, H. (1953) Nature 172, 731–732.
27 Schwan, H.P. (1957) Adv. Biol. Med. Phys. 5, 148–206.
28 Pethig, R. (1979) Dielectric and Electronic Properties of Biological Materials, John Wiley and Sons, Chichester.
29 Glaser, R. (1986) Biophysik, Gustav Fischer Verlag, Stuttgart.
30 Arnold, W.M. and Zimmermann, U. (1982) Z. Naturforsch. 37c, 908–915.
31 Arnold, W.M. and Zimmermann, U. (1988) J. Electrost. 21, 151–191.
32 Arnold, W.M., Schmutzler, R.K., Schmutzler, A.G., Van der Ven, H., Al-Hasani, S., Krebs, D. and Zimmermann, U. (1987) Biochim. Biophys. Acta 905, 454–464.
33 Arnold, W.M., Schmutzler, R.K., Al-Hasani, S., Krebs, D. and Zimmermann, U. (1989) Biochim. Biophys. Acta 979, 142–146.
34 Bertl, A., Felle, H. and Bentrup, F.-W. (1984) Plant Physiol. 76, 75–78.
35 Homblé, F. (1987) Plant Physiol. 84, 433–437.
36 Homblé, F., Ferrier, J.M. and Dainty, J. (1987) Plant Physiol. 83, 53–57.
37 Lühring, H. (1986) Protoplasma 133, 19–28.
38 Sakano, K. and Tazawa, M. (1986) Protoplasma 131, 247–249.
39 Schefczik, K., Simonis, W. and Schiebe, M. (1983) Plant Physiol. 72, 368–375.
40 Bates, G.W., Goldsmith, M.H.M. and T.H. Goldsmith (1982) J. Membr. Biol. 66, 15–23.
41 Barbier-Brygoo, H., Renaudin, J.-P., Manigault, P., Mathieu, Y., Kurkdjian, A. and Guern, J. (1986) in Plant vacuoles, their importance in solute compartmentation in cells and their applications in plant biotechnology, Plenum Press, New York.
42 Bartkoviak, R.A. (1985) Electric circuit analysis, Harper and Row, New York.
43 Simonyi, K. (1979) Theoretische Elektrotechnik, VEB Deutscher Verlag der Wissenschaften, Berlin.